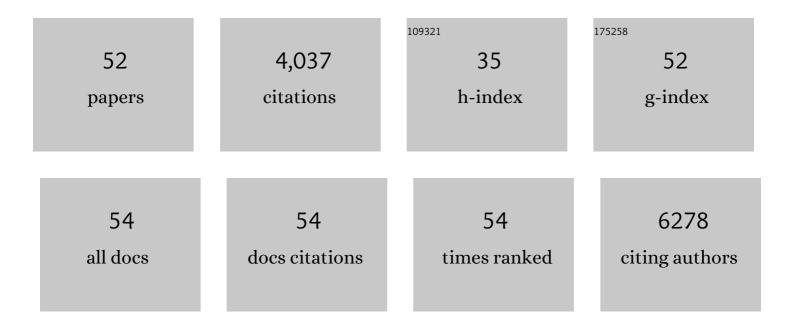
Yih Hong Lee

List of Publications by Year in descending order

Source: https://exaly.com/author-pdf/8076319/publications.pdf Version: 2024-02-01



#	Article	IF	CITATIONS
1	Noninvasive and Point-of-Care Surface-Enhanced Raman Scattering (SERS)-Based Breathalyzer for Mass Screening of Coronavirus Disease 2019 (COVID-19) under 5 min. ACS Nano, 2022, 16, 2629-2639.	14.6	71
2	Tunable Plasmonic Metacrystals: Self-assembly, Plasmonic Properties, and Applications in Surface-enhanced Raman Scattering. , 2022, , 175-232.		0
3	Incorporating plasmonic featurization with machine learning to achieve accurate and bidirectional prediction of nanoparticle size and size distribution. Nanoscale Horizons, 2022, 7, 626-633.	8.0	6
4	Enantiospecific Molecular Fingerprinting Using Potential-Modulated Surface-Enhanced Raman Scattering to Achieve Label-Free Chiral Differentiation. ACS Nano, 2021, 15, 1817-1825.	14.6	29
5	Surface-Enhanced Raman Scattering (SERS) Taster: A Machine-Learning-Driven Multireceptor Platform for Multiplex Profiling of Wine Flavors. Nano Letters, 2021, 21, 2642-2649.	9.1	66
6	Modulating Orientational Order to Organize Polyhedral Nanoparticles into Plastic Crystals and Uniform Metacrystals. Angewandte Chemie - International Edition, 2020, 59, 21183-21189.	13.8	7
7	Modulating Orientational Order to Organize Polyhedral Nanoparticles into Plastic Crystals and Uniform Metacrystals. Angewandte Chemie, 2020, 132, 21369-21375.	2.0	3
8	Applying a Nanoparticle@MOF Interface To Activate an Unconventional Regioselectivity of an Inert Reaction at Ambient Conditions. Journal of the American Chemical Society, 2020, 142, 11521-11527.	13.7	26
9	Two-Photon-Assisted Polymerization and Reduction: Emerging Formulations and Applications. ACS Applied Materials & amp; Interfaces, 2020, 12, 10061-10079.	8.0	47
10	Multiplex Surface-Enhanced Raman Scattering Identification and Quantification of Urine Metabolites in Patient Samples within 30 min. ACS Nano, 2020, 14, 2542-2552.	14.6	87
11	Triboelectrically boosted SERS on sea-urchin-like gold clusters facilitated by a high dielectric substrate. Nano Energy, 2019, 64, 103959.	16.0	23
12	Three-Dimensional Surface-Enhanced Raman Scattering Platforms: Large-Scale Plasmonic Hotspots for New Applications in Sensing, Microreaction, and Data Storage. Accounts of Chemical Research, 2019, 52, 1844-1854.	15.6	94
13	Designing surface-enhanced Raman scattering (SERS) platforms beyond hotspot engineering: emerging opportunities in analyte manipulations and hybrid materials. Chemical Society Reviews, 2019, 48, 731-756.	38.1	468
14	Favoring the unfavored: Selective electrochemical nitrogen fixation using a reticular chemistry approach. Science Advances, 2018, 4, eaar3208.	10.3	333
15	Aluminum nanostructures with strong visible-range SERS activity for versatile micropatterning of molecular security labels. Nanoscale, 2018, 10, 575-581.	5.6	47
16	Probing Plasmon-NV ⁰ Coupling at the Nanometer Scale with Photons and Fast Electrons. ACS Photonics, 2018, 5, 324-328.	6.6	24
17	Creating two self-assembly micro-environments to achieve supercrystals with dual structures using polyhedral nanoparticles. Nature Communications, 2018, 9, 2769.	12.8	46
18	Shape-dependent thermo-plasmonic effect of nanoporous gold at the nanoscale for ultrasensitive heat-mediated remote actuation. Nanoscale, 2018, 10, 16005-16012.	5.6	19

Yih Hong Lee

#	Article	IF	CITATIONS
19	Dynamic Rotating Liquid Marble for Directional and Enhanced Mass Transportation in Three-Dimensional Microliter Droplets. Journal of Physical Chemistry Letters, 2017, 8, 243-249.	4.6	22
20	Direct Metal Writing and Precise Positioning of Gold Nanoparticles within Microfluidic Channels for SERS Sensing of Gaseous Analytes. ACS Applied Materials & Interfaces, 2017, 9, 39584-39593.	8.0	42
21	Flexible Three-Dimensional Anticounterfeiting Plasmonic Security Labels: Utilizing <i>Z</i> -Axis-Dependent SERS Readouts to Encode Multilayered Molecular Information. ACS Photonics, 2017, 4, 2529-2536.	6.6	44
22	Constructing Soft Substrate-less Platforms Using Particle-Assembled Fluid–Fluid Interfaces and Their Prospects in Multiphasic Applications. Chemistry of Materials, 2017, 29, 6563-6577.	6.7	11
23	Driving CO ₂ to a Quasi-Condensed Phase at the Interface between a Nanoparticle Surface and a Metal–Organic Framework at 1 bar and 298 K. Journal of the American Chemical Society, 2017, 139, 11513-11518.	13.7	55
24	Tuning Molecular-Level Polymer Conformations Enables Dynamic Control over Both the Interfacial Behaviors of Ag Nanocubes and Their Assembled Metacrystals. Chemistry of Materials, 2017, 29, 6137-6144.	6.7	20
25	Quantitative prediction of the position and orientation for an octahedral nanoparticle at liquid/liquid interfaces. Nanoscale, 2017, 9, 11239-11248.	5.6	11
26	Assembling substrate-less plasmonic metacrystals at the oil/water interface for multiplex ultratrace analyte detection. Analyst, The, 2016, 141, 5107-5112.	3.5	6
27	Localized and Continuous Tuning of Monolayer MoS ₂ Photoluminescence Using a Single Shape ontrolled Ag Nanoantenna. Advanced Materials, 2016, 28, 701-706.	21.0	73
28	A Chemical Approach To Break the Planar Configuration of Ag Nanocubes into Tunable Two-Dimensional Metasurfaces. Nano Letters, 2016, 16, 3872-3878.	9.1	61
29	Identifying Enclosed Chemical Reaction and Dynamics at the Molecular Level Using Shell-Isolated Miniaturized Plasmonic Liquid Marble. Journal of Physical Chemistry Letters, 2016, 7, 1501-1506.	4.6	30
30	Spinning Liquid Marble and Its Dual Applications as Microcentrifuge and Miniature Localized Viscometer. ACS Applied Materials & Interfaces, 2016, 8, 23941-23946.	8.0	33
31	Formulating an Ideal Protein Photoresist for Fabricating Dynamic Microstructures with High Aspect Ratios and Uniform Responsiveness. ACS Applied Materials & Interfaces, 2016, 8, 8145-8153.	8.0	15
32	Nanoscale surface chemistry directs the tunable assembly of silver octahedra into three two-dimensional plasmonic superlattices. Nature Communications, 2015, 6, 6990.	12.8	137
33	Nanoporous Gold Nanoframes with Minimalistic Architectures: Lower Porosity Generates Stronger Surface-Enhanced Raman Scattering Capabilities. Chemistry of Materials, 2015, 27, 7827-7834.	6.7	56
34	Multiplex plasmonic anti-counterfeiting security labels based on surface-enhanced Raman scattering. Chemical Communications, 2015, 51, 5363-5366.	4.1	89
35	Shape-Shifting 3D Protein Microstructures with Programmable Directionality via Quantitative Nanoscale Stiffness Modulation. Small, 2015, 11, 740-748.	10.0	50
36	Plasmonic Liquid Marbles: A Miniature Substrateâ€less SERS Platform for Quantitative and Multiplex Ultratrace Molecular Detection. Angewandte Chemie - International Edition, 2014, 53, 5054-5058.	13.8	86

YIH HONG LEE

#	Article	IF	CITATIONS
37	Hierarchical 3D SERS Substrates Fabricated by Integrating Photolithographic Microstructures and Selfâ€Assembly of Silver Nanoparticles. Small, 2014, 10, 2703-2711.	10.0	169
38	Graphene oxide and shape-controlled silver nanoparticle hybrids for ultrasensitive single-particle surface-enhanced Raman scattering (SERS) sensing. Nanoscale, 2014, 6, 4843-4851.	5.6	206
39	Understanding the Synthetic Pathway of a Single-Phase Quarternary Semiconductor Using Surface-Enhanced Raman Scattering: A Case of Wurtzite Cu ₂ ZnSnS ₄ Nanoparticles. Journal of the American Chemical Society, 2014, 136, 6684-6692.	13.7	129
40	Plasmonic Silver Nanowire Structures for Two-Dimensional Multiple-Digit Molecular Data Storage Application. ACS Photonics, 2014, 1, 631-637.	6.6	43
41	Chemical speciation of heavy metals by surface-enhanced Raman scattering spectroscopy: identification and quantification of inorganic- and methyl-mercury in water. Nanoscale, 2014, 6, 8368-8375.	5.6	92
42	Precision Synthesis: Designing Hot Spots over Hot Spots via Selective Gold Deposition on Silver Octahedra Edges. Small, 2014, 10, 4940-4950.	10.0	36
43	Bimetallic Platonic Janus Nanocrystals. Langmuir, 2013, 29, 12844-12851.	3.5	15
44	Correlating the Plasmonic and Structural Evolutions during the Sulfidation of Silver Nanocubes. ACS Nano, 2013, 7, 9354-9365.	14.6	57
45	Vertically Aligned Gold Nanorod Monolayer on Arbitrary Substrates: Self-Assembly and Femtomolar Detection of Food Contaminants. ACS Nano, 2013, 7, 5993-6000.	14.6	218
46	Using the Langmuir–Schaefer technique to fabricate large-area dense SERS-active Au nanoprism monolayer films. Nanoscale, 2013, 5, 6404.	5.6	69
47	Superhydrophobic Surface-Enhanced Raman Scattering Platform Fabricated by Assembly of Ag Nanocubes for Trace Molecular Sensing. ACS Applied Materials & Interfaces, 2013, 5, 11409-11418.	8.0	110
48	Enhanced Optical Properties of Graphene Oxide–Au Nanocrystal Composites. Langmuir, 2012, 28, 321-326.	3.5	73
49	A Chemical Route To Increase Hot Spots on Silver Nanowires for Surface-Enhanced Raman Spectroscopy Application. Langmuir, 2012, 28, 14441-14449.	3.5	84
50	Plasmon enhanced upconversion luminescence of NaYF4:Yb,Er@SiO2@Ag core–shell nanocomposites for cell imaging. Nanoscale, 2012, 4, 5132.	5.6	250
51	Refractive Index Sensitivities of Noble Metal Nanocrystals: The Effects of Multipolar Plasmon Resonances and the Metal Type. Journal of Physical Chemistry C, 2011, 115, 7997-8004.	3.1	113
52	Nonlinear optical switching behavior of Au nanocubes and nano-octahedra investigated by femtosecond Z-scan measurements. Applied Physics Letters, 2009, 95, .	3.3	89